ISSN 1070-4272, Russian Journal of Applied Chemistry, 2013, Vol. 86, No. 12, pp. 1885−1896. © Pleiades Publishing, Ltd., 2013.
Original Russian Text © V.V. Dolgov, N.R. Ashurov, E.E. Sheveleva, E.O. Khakberdiev, 2013, published in Zhurnal Prikladnoi Khimii, 2013, Vol. 86, No. 12, pp. 1938−1949.

MACROMOLECULAR COMPOUNDS AND POLYMERIC MATERIALS

Strength-Strain, Barrier, Thermal, and Fire-Resistance Properties of Nanocomposites Based on Linear Polyethylene with Montmorillonite

V. V. Dolgov, N. R. Ashurov, E. E. Sheveleva, and E. O. Khakberdiev

Institute of Polymer Chemistry and Physics, Academy of Sciences of the Republic of Uzbekistan, Tashkent, Uzbekistan
e-mail: dolgov.valentin@gmail.com

Received December 5, 2013

Abstract—Strength-strain, sorption, thermal, and fire-resistance properties of nanocomposites based on linear low-density polyethylene with montmorillonite modified with a quaternary phosphonium salt were studied. It is shown that the diffusion, sorption, and permeability of the nanocomposites depends on the type of a montmorillonite and its concentration in the polymer, and also on the nature of a penetrant and degree of its thermodynamic affinity for the polymer. Introduction of up to 3 wt % organomontmorillonite improves the thermal stability by more than 90°, raises the oxygen index to 20 vol %, and makes the elastic modulus 47% larger relative to the base polymer due to the nanostructural morphology formed in the course of mixing.

DOI: 10.1134/S1070427213120148

Filling of polymers with various fillers improves their performance to a certain extent. Introduction of coarsely dispersed inorganic particles (40–80 wt %) into polymers leads to an increase (by 30–40%) of the elastic modulus and thermal and fire-resistance properties. At the same time, a diverse effect of such a strong filling is also observed: the rheological characteristics are impaired, which has a negative effect in the course of the processing by leading to an increase in the mass and density of a finished article, loss of plasticity, and embrittlement of the material.

An integrated improvement of the properties of a polymeric material (without loss of its characteristic properties) is, in principle, only possible upon introduction of nanosize particles of varied nature and shape into the polymer matrix. This was demonstrated for the example of polymeric nanocomposites based on thermoplastics filled with a layered aluminosilicate, montmorillonite (MMT) [1]. Polymeric nanocomposites were first produced in 1993 by Japanese researchers from polyamide-6 by the polymerization filling method [2–4]. It was reported in the same year [5] that nanocomposites were obtained in a polymer melt via stratification of montmorillonite with a sandwich-like structure in the polymer matrix to individual layers (exfoliation). Accordingly, a key goal in development of nanocomposites is to reach the maximum extent of exfoliation and a uniform distribution of planar nanoparticles (whose perimeter is 200–400 nm, and thickness, 1 nm) in the polymer matrix. These results provided the basis for similar studies for nearly all large-tonnage polymers of varied nature and chemical structure [6–14].

When nanocomposites are formed on the basis of nonpolar polymers, e.g., polyolefins, certain difficulties are encountered, related to the thermodynamics of compatibility of a polymer and a mineral and to structural specific features of the latter (small interplanar spacing). Introduction of the so-called compatibilizer, which is another polymer or a polyolefin with polar functional groups [15–18], and modification of a hydrophilic filler with ammonium salts [19] (of the R_4N^+ type, where at least one of R is a long-chain aliphatic radical) make it possible to achieve, to a certain extent, the desired results [20–24]. The driving force of the stratification of MMT particles to individual layers is, in addition to the shear field in component mixing, the occurrence of specific interactions of polymer macromolecules both with the hydrophilic layers of the aluminosilicate and with modifier molecules. In this case, the higher the interaction energy, the smaller the number of thermodynamic obstacles to formation of nanostructures [25–29].

Thus, polymeric materials with good mechanical [30, 31], thermal [20], and fire-resistance [32, 33] characteristics can be obtained by their filling with a small amount (1–10 wt %) of layered aluminosilicate nanoparticles.

It is known that polyethylene has a low deformation heat-resistance and is subject to oxidative aging. The fast inflammation of the polymer and its intense combustion lead to fire hazard. The filling of polyethylene with montmorillonite, followed by formation of nanostructures of various types, can strongly improve the heat resistance and retard the combustion of a material. By virtue of their improved characteristics, nanocomposites can find use as engineering (including those of the structural type) and electrical-engineering materials and consumer goods, such as, e.g., hot-water supply tubes (instead of polypropylene), automobile particles, and construction materials.

The goal of our study was to examine specific features of how nanocomposites based on linear low-density polyethylene with organophilic montmorillonite are formed and their structural parameters are related to the strength-strain, thermal, barrier, and fire-resistance properties.

EXPERIMENTAL

We used linear low-density polyethylene (PE, ρ = 0.920 g cm^{-3}, F-0220 brand, Shurtan gas-chemical complex of the Republic of Uzbekistan), sodium montmorillonite (Na-MMT, d_{001} = 1.248 Å, cation-exchange capacity 90 mg-equiv/100 g, Zhangjiakou Qinghe Chemical Factory, China), maleinized polyethylene (MAPE) based on the above polyethylene with 45 wt % grafted maleic anhydride (laboratory product) as compatibilizer [34], and montmorillonite modified with P,P',P''-triphenyl-P'''-octadecylphosphonium bromide $[(C_{18}H_{37})(C_6H_5)_3P]+Br-$ (P-MMT).The modifier concentration in P-MMT was 29.7 wt % (laboratory product) [35].

The components were mixed in a HAAKE Reomex OS PTW16 double-screw extruder (*L*/*D* = 40, *D* = 16 mm) *t* 60 rpm in the temperature range 185–210°C. Polymeric composites were obtained on the basis of two matrices: polyethylene and a PE/MAPE polymer-polymer mixture (in a 80/20 wt % ratio). The content of MMT in all the composites was 3 wt %.

An X-ray structural analysis of the polymeric composites was made on a Rigaku D/max 2400 X-ray diffractometer with CuKα radiation (λ = 1.54056 Å) at a recording rate of 2 deg min^{-1}. The morphology of the composites was studied with a Hitachi H-800 transmission electron microscope at an accelerating voltage of 100 kV. Tensile disintegration tests were performed with an Instron 3365 tensile machine at a deformation rate of 50 mm min^{-1} (ASTM D638). Sorption tests were carried out in three penentrants: benzene (C_6H_6), dichloromethane (CH_2Cl_2), and pentane (C_5H_{12}), with the results obtained used to calculate the diffusion, sorption, and permeation coefficients [GOST (State Standard) 12020]. The fire-resistance of the samples was evaluated by the oxygen index method (ASTM D2863) and by the fire propagation rate parameter (UL 94HB, ASTM D635). Samples for the tests were cast in the form of blades (2 mm thick), disks (10 mm in diameter, 2 mm thick), and bars (125 × 10 × 0.4 mm) from granules on a HAAKE MiniJet II injection machine at a temperature of 200°C and pressure of 5 atm.

The thermal stability of the samples was determined by thermogravimetry on a Perkin Elmer Pyris TGA instrument in the temperature range 50–700°C (heating rate 10 deg min^{-1}) in the atmospheres of nitrogen and air. The melting point and the heat of melting (or crystallization) of the samples were measured with a Perkin Elmer DSC 7 differential scanning calorimeter in the temperature range 25–150°C (heating rate 20 deg min^{-1}) in the heating–cooling–heating mode in air.

The coke number was determined by pyrolysis of the samples in a muffle furnace for 2 min at a temperature of 850°C. The melt flow index (MFI) of the polymers and composites on their basis was determined at a temperature of 190°C under loads of 2.16 and 5.0 kg (ASTM D1238).

RESULTS AND DISCUSSION

It is known [12] the morphology of a polymer/montmorillonite composite is nonuniform and has

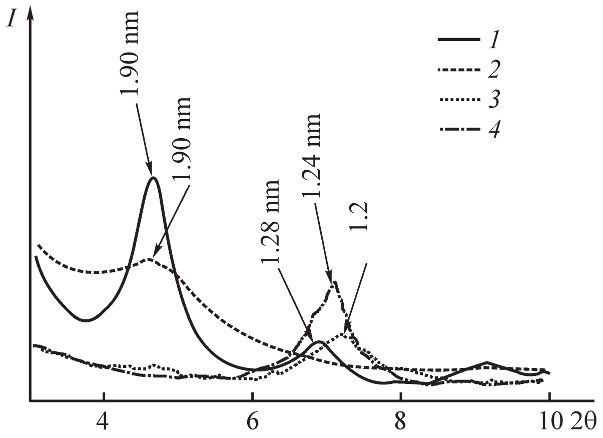

Fig. 1. X-ray diffraction patterns of composites, measured in the reflection configuration. (*1*) PE/P-MMT, (*2*) PE/MAPE/P-MMT, (*3*) PE/Na-MMT, and (*4*) PE/MAPE/Na-MMT.

the form of a mixture of four structural types formed in the polymeric matrix (nonintercalated, intercalated, intercalated-flocculated, and exfoliated structures) and predominance of one of these determines, in the end, its properties. As already noted, the role of the driving force for formation of a preferentially intercalated and exfoliated nanostructures is played by certain conditions: chemical nature of a modifier and its concentration in MMT, chemical nature of the compatibilizer and degree of its functionality, concentrations of a filler and compatibilizer in the polymeric matrix, and mixing conditions (shear rate and time).

Figure 1 shows X-ray diffraction patterns of composites and nanocomposites with 3 wt % MMT of two types with different polarities. It can be seen that both in the absence and in the presence of the compatibilizer, no intercalation of Na-MMT occurs, which is indicated by the fixed 001 reflection at a diffraction angle 2θ = 7.12° (*d* = 1.24 nm), whose position is identical to that of the reflection for Na-MMT not mixed with the polymer.

A halo with a weak peak (with a smaller area under the curve) at 4.64° (*d* = 1.90 nm) is indicative of a substantial exfoliation, whereas the intercalated fraction of P-MMT is also present in the PE/MAPE/P-MMT nanocomposite. The position of this peak is comparable with that for the PE/P-MMT microcomposite. The peaks for these two compositions are shifted to smaller scattering angles 2θ relative to the reflection for P-MMT not mixed with the polymer (5.20°, *d* = 1.69 nm).

The X-ray diffraction data are in a rather good agreement with the results furnished by transmission electron microscopy (TEM).

Figure 2 shows TEM micrographs of the morphology of composites with two kinds of montmorillonite in the presence of the MAPE compatibilizer.

The micrographs in Fig. 2a show both intercalated and exfoliated P-MMT particles with a thickness of less than 5 nm in the longitudinal direction. Coarse aggregates of Na-MMT particles with transverse sizes of 0.1 to 1.0 μm can be seen in Fig. 2b.

An important issue in development of nanocomposites is the enhancement of the stress-strain properties of a polymer, which are, in turn, determined by the morphology of the nanocomposite, degree of crystallinity and orientation of polyethylene lamellas,

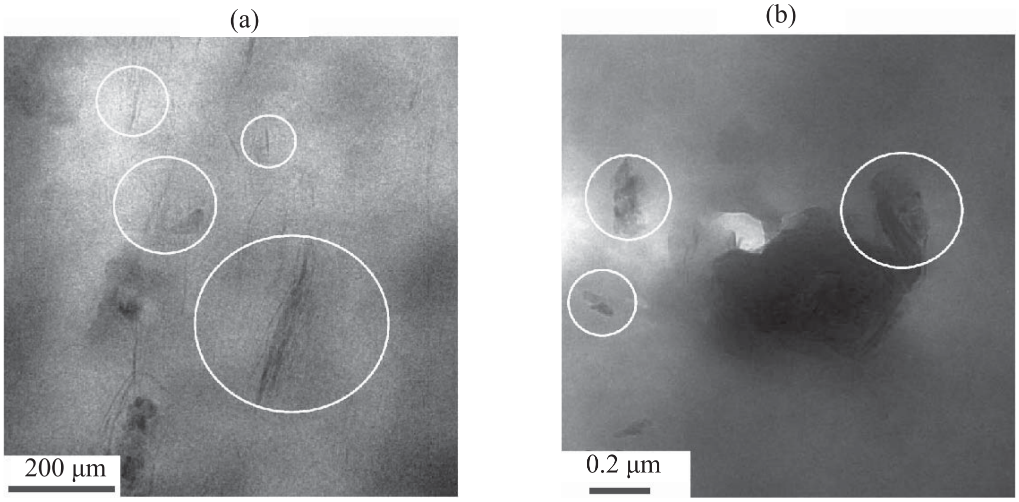

Fig. 2. Micrographs of the morphology of composites based on PE/MAPE with (a) P-MMT or (b) Na-MMT.

Table 1. Stress-strain characteristics of polyethylene and composites on its basis

Sample no.	Composition	σ_{tens}	σ_y	σ_{br}	ε, %	*E*, MPa
		MPa				
1	PE	16.1 ± 1.3	13.7 ± 1.2	14.1 ± 2.5	743 ± 73	95 ± 11
2	PE/P-MMT	15.7 ± 1.7	14.4 ± 1.5	11.5 ± 1.8	717 ± 42	109 ± 7
3	PE/Na-MMT	16.5 ± 1.8	13.2 ± 1.4	13.9 ± 1.5	747 ± 46	100 ± 5
4	PE/MAPE	16.8 ± 1.3	16.8 ± 1.3	7.9 ± 1.1	105 ± 21	116 ± 5
5	PE/MAPE/P-MMT	18.3 ± 1.3	18.3 ± 1.3	11.9 ± 1.8	92 ± 10	140 ± 3
6	PE/MAPE/Na-MMT	18.0 ± 1.9	18.0 ± 1.9	10.5 ± 1.8	103 ± 16	117 ± 5

molecular mass and molecular-mass distribution of the matrix polymer, and physical and chemical interactions of the polymer with filler nanoparticles [15, 30, 32, 36, 37].

Table 1 lists the stress-strain parameters of the composites: tensile strength σ_{tens} at the yield σ_y and breaking stress σ_{br}, relative elongation at break ε, and Young's modulus *E*.

It can be seen in Table 1 that σ_{br} for the PE/MAPE composite becomes 1.8 times lower than that of the starting polyethylene, with a slight increase in *E* (by 22%), and ε decreases by a factor of 21. However, the breaking stress of the polymer-polymer mixture compares well with that for polyethylene.

The strength properties of sample nos. 2 and 3 with Na-MMT and P-MMT do not differ so significantly from the properties of the base polymer, whereas their elasticity modulus increases by 5 and 15%, respectively.

The presence of the compatibilizer in the matrix of the nonpolar polymer promotes adhesion interactions between the incompatible dispersed and dispersion phases. For example, the σ_{br} of composite no. 6 increases by 33% as compared with the PE/MAPE mixture.

Comparatively better parameters are observed for composite no. 5 with P-MMT, whose breaking stress is 1.5 times that for PE/MAPE composites and compares well with the strength parameter of unfilled polyethylene. At the same time, *E* increases by 21% relative to that of the unfilled PE/MAPE composition, or by 47% relative to the unfilled polymer, which the largest value among all the compositions. The value of ε for the given composition remains unchanged relative to the PE/MAPER polymer-polymer mixture, but is 8 times lower than that of unfilled polyethylene, which is indicative of the loss of elasticity by the nanocomposite.

Compared with the starting polymer, the nanocomposites have a substantially lower permeability to gases, such as CO_2, N_2, and O_2 [38–40]. However, the condensed state of a penetrant (sorbate) and its chemical nature affect in a somewhat different way the sorption properties of the nanocomposites.

Figure 3 shows physical sorption isotherms of pentane (C_5H_{12}), dichloromethane (CH_2Cl_2), and benzene (C_6H_6) by polyethylene and composites on its basis. The changes in the sorption parameters may be due to the partial loss of crystallinity by the polymer, concentration of an aluminosilicate and its chemical nature, degree of exfoliation and layer orientation on the polymer matrix, chemical nature of a modifier and penetrant, and specific interactions of the penetrant–aluminosilicate and penetrant–organomodifier types.

The tendency in variation of the diffusion (*D*), sorption (*S*), and permeability (*P*) parameters with the types of a penetrant and an MMT and with the polarity of polymers is reflected in Table 2. Let us consider the following three interrelated physical phenomena.

Diffusion. In polymers, the diffusion of a gas or a fluid occurs due to the thermal motion of segments of macromolecules in the diffusion medium. In this case, substance is transferred from the high-concentration region to that with low concentration and the system passes from the nonequilibrium state to that in equilibrium. The diffusion of a substance occurs in the free volume (intermolecular spaces of various shapes and

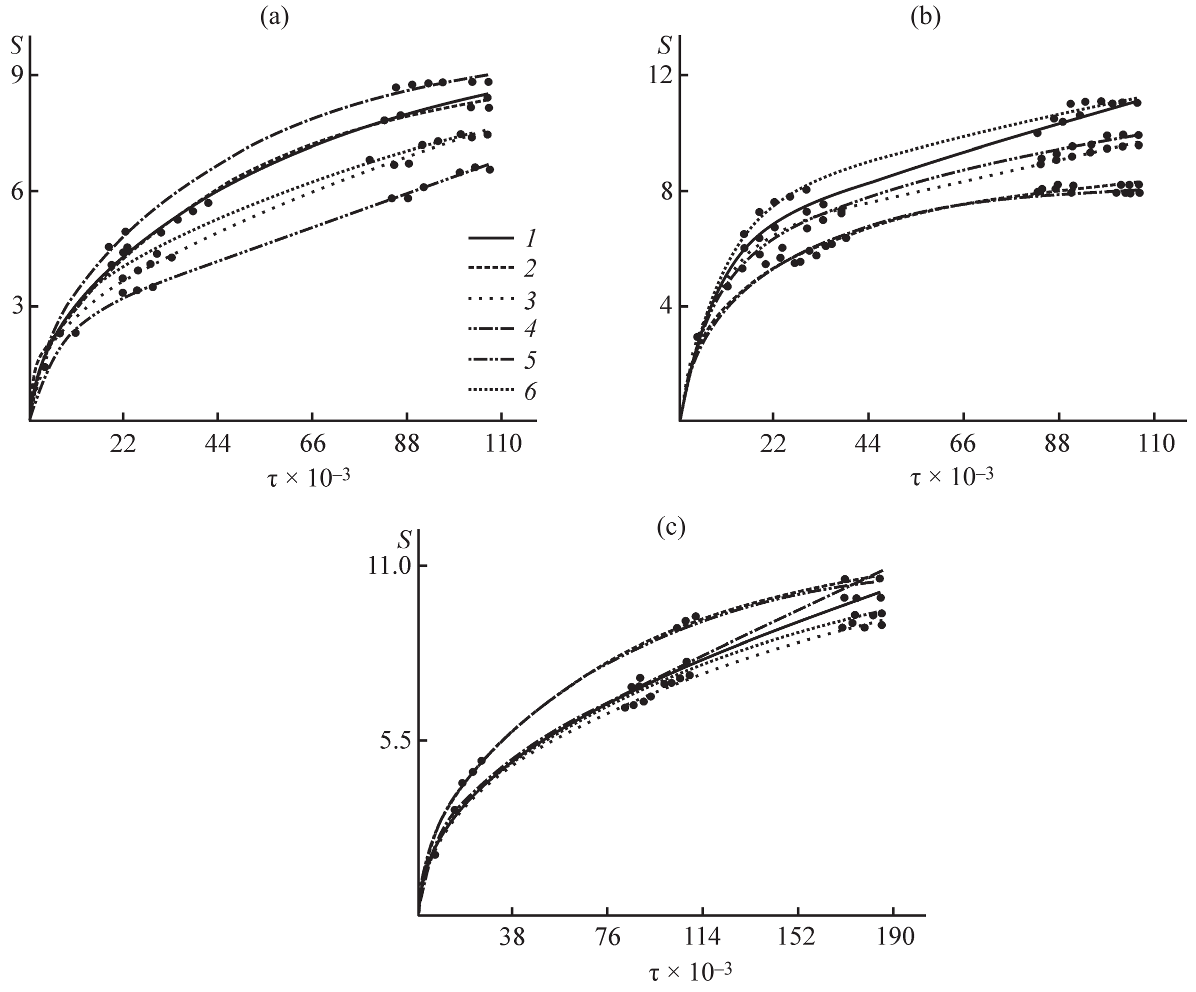

Fig. 3. Sorption isotherms of composites for three penetrants: (a) CH_2Cl_2, (b) C_5H_{12}, and (c) C_6H_6. (*1*) PE, (*2*) PE/MAPE, (*3*) PE/Na-MMT, (*4*) PE/P-MMT, (*5*) PE/MAPE/Na-MMT, and (*6*) PE/MAPE/P-MMT.

sizes) in the polymer, i.e., with periodic displacement of diffusing molecules from one equilibrium state into another, or from volume into another [41].

For the starting polymer and the polymer-polymer mixture (sample nos. 1 and 4), *D* varies with the penetrant type (aliphatic, halide-aliphatic, and aromatic) in the following order: $CH_2Cl_2 > C_5H_{12} > C_6H_6$. Compared with the starting polyethylene, the presence of the phosphonium modifier in P-MMT leads to a certain increase in *D*, especially for CH_2Cl_2 (sample no. 2). For the composition with Na-MMT, *D* somewhat decreases for C_5H_{12} and increases for CH_2Cl_2 and C_6H_6 as compared with microcomposite no. 2.

Compared with the PE/MAPE composition, nanocomposite no. 5 shows no significant changes in *D*. As expected, the diffusion parameter of microcomposite no. 6 with Na-MMT for C_6H_{12} and CH_2Cl_2 is somewhat smaller than that for C_6H_6.

Sorption. It can be seen in Table 1 that the penetrant sorption coefficient decreases for PE in the order $CH_2Cl_2 > C_6H_6 > C_5H_{12}$. Compared with polyethylene, the sorption of C_6H_6 by P-MMT is at a maximum, whereas that by the composite with Na-MMT is at a minimum, as also that for the rest of the sorbates. In the case of the polymer mixture, the sorption of C_6H_6 is the highest. However, the sorption of CH_2Cl_2 by composite no. 5 is the highest, and that of C_5H_{12} by composite no. 6 is the lowest.

It is reasonable that the sorption of hydrophilic penetrants will decrease with increasing fraction of the aluminosilicate for a hydrophobic or organophilic filler (P-MMT) or increase in the case of a hydrophilic filler

(Na-MMT). It is noteworthy that the content of Na-MMT is 3 wt %, and that of the base aluminosilicate in P-MMT, only about 2 wt % (because the rest of the mass is accounted for by the modifier).

Permeability. The permeability of polyethylene to the penetrants grows in the order $CH_2Cl_2 > C_5H_{12} > C_6H_6$. This tendency is preserved both for polyethylene-based nanocomposite nos. 2 and 3 and for nanocomposite no. 5, based on the polymer-polymer mixture. However, no significant difference in *P* values is observed for the composites and the unfilled polymer.

Possibly, the small degree of filling results in that the sorption properties only slightly depend on the nanocomposite structure under liquid/solid test conditions. However, the results obtained suggest that the sorption, diffusion, and permeability of fatty penetrants decrease in the presence of a certain fraction of a polar agent (compatibilizer or filler) in the electrolytes-based composite; with increasing fraction of MMT in the polymer, the sorption processes are hindered by the barrier effect. As a result of the insignificant changes in the sample size and according to sorption data, the penetrants used cause a limited swelling of both the polymer and composites on its basis.

It is known that processes of polymer crystallization and recrystallization are affected by the nature, size,

Table 2. Diffusion, sorption, and permeability coefficients for the polymer and polymeric composites

Sample no.	Composition	$D \times 10^{-7}$, cm^2 s^{-1}			$S \times 10^{-2}$, g cm^{-3}			$P \times 10^{-8}$, cm^2 g^{-1} s^{-1} cm^{-3}		
		C_5H_{12}	CH_2Cl_2	C_6H_6	C_5H_{12}	CH_2Cl_2	C_6H_6	C_5H_{12}	CH_2Cl_2	C_6H_6
1	PE	3.73	5.96	1.99	7.40	9.83	8.95	2.76	5.86	1.79
2	PE/P-MMT	4.32	7.32	1.95	7.97	7.16	9.34	3.44	5.24	1.82
3	PE/Na-MMT	3.39	7.66	2.17	6.61	8.82	8.27	2.25	6.75	1.79
4	PE/MAPE	3.96	7.32	2.49	7.32	7.39	9.69	2.89	5.41	2.41
5	PE/MAPE/P-MMT	4.28	6.95	2.11	7.45	10.29	8.69	2.89	7.15	1.84
6	PE/MAPE/Na-MMT	3.28	6.67	2.61	5.89	9.39	9.59	1.93	6.26	2.50

Table 3. Melting point and heat of melting (crystallizatin) and degree of crystallinity of polymers and composites on their basis

Sample no.	Composition	mp, °C		ΔH_m, J g^{-1}	T_{cr}, °C	ΔH_{cr}, J g^{-1}	χ, %
		T_1	T_2				
1	PE	117.6	–	110.12	99.4	–78.29	37.6
2	MAPE	106.3	–	74.75	81.2	–47.50	25.5
3	PE/MAPE	121.3	106.9	92.85	111.9	–88.46	31.7
4	PE/P-MMT	121.1	109.0	122.90	108.3	–131.27	43.2
5	PE/MAPE/P-MMT	120.9	105.6	81.02	111.9	–73.63	28.5
6	PE/Na-MMT	121.0	109.0	105.18	107.9	–125.37	37.0
7	PE/MAPE/Na-MMT	120.9	105.6	91.87	110.5	–81.52	32.3

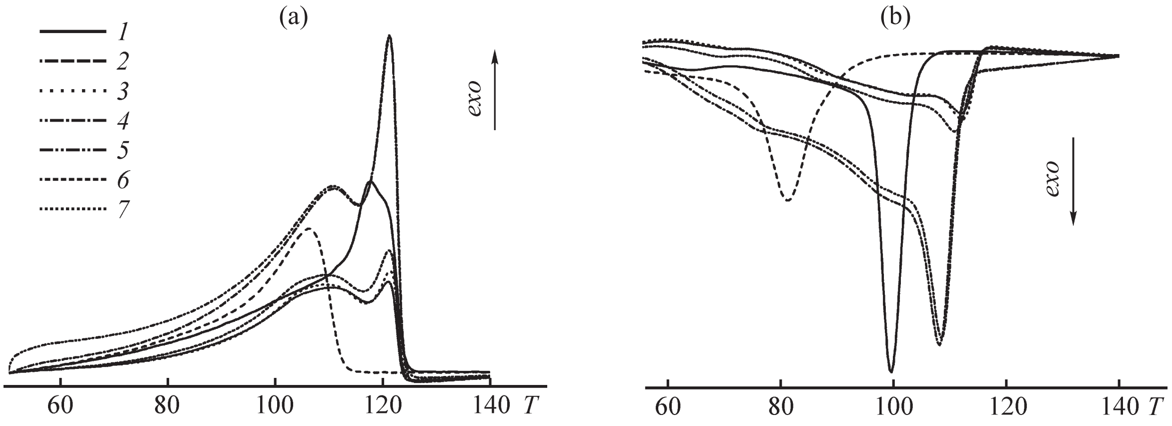

Fig. 4. DSC curves for (a) melting and (b) crystallization of polymers and polymeric composites. (*1*) PE, (*2*) MAPE, (*3*) PE/MAPE, (*4*) PE/Na-MMT, (*5*) PE/P-MMT, (*6*) PE/MAPE/Na-MMT, and (*7*) PE/MAPE/P-MMT.

shape, and concentration of filler particles. Figure 4a shows melting endotherms of PE and MAPE. The melting peaks of these polymers lie at 117.6 and 106.3°C, respectively. The additional amorphization of MAPE is probably due to the steric factor: presence of maleic anhydride groups in MAPE prevents chains from being packed into a crystal lattice similar to that of polyethylene, which leads to "loosening" of the supramolecular structure and to the resulting decrease in the melting point. This is confirmed by the decrease in the degree of crystallinity ($\Delta\chi$PE – $\Delta\chi$MAPE = 12.1%) and by the shift of the endothermic melting peak of MAPE to lower temperatures (mpPE – mpMAPE = 11.3°C).

The melting curve of the polymer–polymer mixture shows two poorly pronounced peaks (Fig. 4a) at slightly higher temperatures (Fig. 4, Table 3). Despite that their degree of crystallinity is comparatively similar to that of PE, PE/MAPE presumably contains a substantially smaller amount of perfect-shape crystals.

There is no significant difference between the positions of the endothermic peaks in polyethylene-based compositions with 3 wt % Na-MMT or P-MMT. However, sample no. 4 has comparatively high values of ΔH_{melt} (122.90 J g^{-1}) and χ (43.2%), compared with the unfilled polymer and sample no. 6 (Fig. 4, Table 3).

Two peaks are pronounced in the DCS curves of microcomposite nos. 4 and 6 (it is noteworthy that, in this case, the recrystallization results in that a single peak is formed in the first stage of heating, and a doublet, in the second stage. The peak at 105–115°C is probably due to the melting of less perfect crystallites, as, e.g., in the case of the polymer-polymer mixture. The second peak at 115–125°C is associated with the melting of polyethylene crystallites with more ideal shape and structure [42]. In this case, MMT particles can serve as crystallization nuclei and, without affecting the total degree of crystallinity of the composite, be involved in the formation of a polyethylene crystal structure of a perfect type.

It can be seen in Table 3 that presence of any kind of MMT in the PE/MAPE matrix (sample nos. 5 and 7) hardly affects the melting and crystallization points. However, χ of sample no. 5 decreases by 3.2% relative to χ of sample nos. 1 and 7. It is quite probable that the crystallization is hindered to a full extent on exfoliated aluminosilicate particles because of the formation of new surfaces and specific interactions between active centers of the aluminosilicate and maleic anhydride in PEMA. Table 3 lists, according to DSC data, the melting points and heats of melting, and also the crystallization points and heats of crystallization for polymers and composites on their basis.

Undoubtedly, the resistance of nanocomposites against thermo-oxidative aging is determined not only by the polymer structure, but also by the type of structures formed by MMT in the polymer. For example, a slight difference in the loss of mass, compared with the unfilled polymer, is observed for the microcomposite of PE/P-MMT composition (with a weakly intercalated structure): $\Delta T_{5\%}$ = 3°C and $\Delta T_{10\%}$ = 6°C (Table 4). A larger difference in the loss of mass is observed for the PE/MAPE/P-MMT nanocomposite and the polymer-polymer mixture and polyethylene. Even at a 10%

Table 4. Melt flow index, coke number, and thermal and fire-resistance properties of polymers and composites on their basis

Sample no.	Composition	Temperature of indicated loss of mass, °C						Coke number, %	ν, mm min^{-1}	OI, vol %	MFI, g/10 min	
		air			nitrogen							
		5%	10%	50%	5%	10%	50%				2.16 kg	5.00 kg
1	PE	317	341	391	446	458	480	0.14	23.8	18.0	2.00	–
2	MAPE	291	352	438	391	444	476	0.14	–	–	–	–
3	PE/MAPE	291	332	410	–	–	–	0.14	35.6	18.5	0.10	0.50
4	PE/P-MMT	320	347	415	446	458	483	6.79	24.6	18.5	1.90	5.40
5	PE/MAPE/P-MMT	305	382	437	448	460	485	4.24	23.6	20.0	0.10	0.57
6	PE/Na-MMT	307	338	397	452	462	484	1.69	26.5	18.0	2.10	5.60
7	PE/MAPE/ Na-MMT	297	339	414	445	456	481	1.64	35.4	18.0	0.50	1.85

loss of mass, Δ*T* is 50°C relative to PE/MAPE or 41°C relative to polyethylene.

Portion *I* in the TG curves of the nanocomposite with P-MMT and microcomposite with Na-MMT in Figs. 5a and 5b (in the atmosphere of air) shows the duration of the thermo-oxidative destruction in the temperature range 250–450°C in comparison with the unfilled polymers. The physical mechanism of the influence exerted by Planar MMT particles consists in hindering the diffusion of oxygen (Fig. 5, portion *I*) into the polymer melt, with the deficiency of oxygen, in turn, changing the direction and decelerating the destructive processes.

The hindrance to the diffusion of oxygen and the occurrence of chain-termination reactions depend both on the concentration of the aluminosilicate and on the degree of its exfoliation in the polymer. The active loss of mass, compared with that by the base polymer, occurs at 422.8°C ($\Delta T = 91.3$°C) for the nanocomposite with P-MMT and at 396.5°C ($\Delta T = 65$°C) for the microcomposite with Na-MMT. According to the results of [43], oxygen is sorbed by the polymer melt from the atmosphere in the early stage of the thermo-oxidative destruction and is localized at active centers of the aluminosilicate. In turn, these centers initiate disproportionation reactions (rupture of a C–H bond and formation of a C macroradical). The macroradicals interact with oxygen and(or) recombine. In the end, the competing reactions of disproportionation and recombination in the presence of the aluminosilicate result in the structuring of the polymer (as a basis for coke formation), now under the high-temperature pyrolysis conditions.

Portion *II*, which is not observed in the TG curves of composites analyzed in an inert atmosphere, show the region of coke formation, with a low content of coke being characteristic of the unfilled polyethylene, and a higher content, of a nanocomposite (Table 4).

Coke starts to be formed at high temperatures for the nanocomposite with P-MMT earlier as compared with the identical composition with Na-MMT (comparative data for portion *II*). The loss of mass in the temperature range 450–550°C in the given portion is due to the slow oxidation of the coke (Fig. 5, Table 4).

It can be seen in Table 4 that there is no difference in temperatures in the initial stages of thermo-oxidative destruction of MAPE and PE/MAPE, but, compared with the unfilled polyethylene, their destruction begins noticeably earlier. In the initial stage, oxygen diffusing into the polymer melt initiates disproportionation reactions and formation of hydroperoxides, which, in turn, decompose at high temperatures to give more mobile HO radicals. In this case, an increase in the concentration of these latter in the polymer makes the thermo-oxidative destruction faster.

The active thermal destruction of polyethylene begins in an inert atmosphere at 463°C and is accompanied by

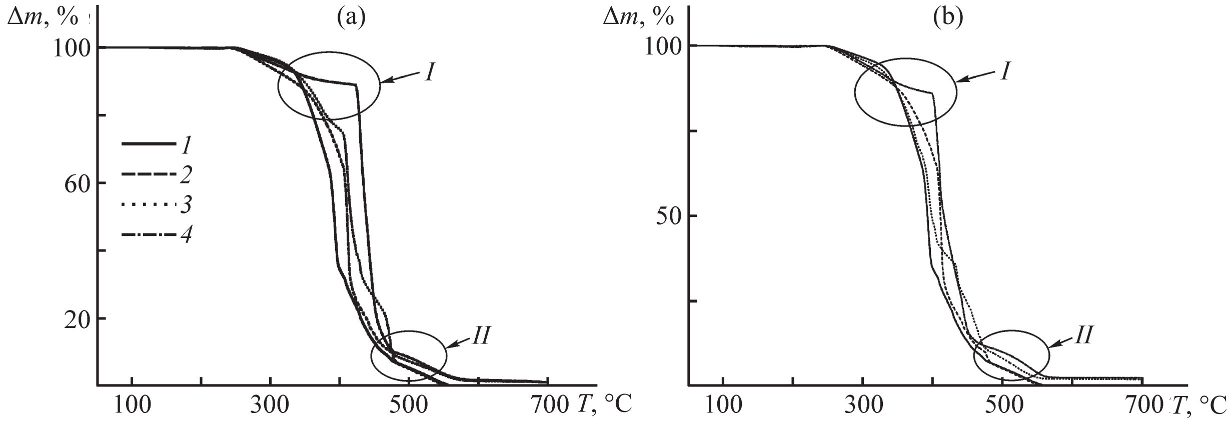

Fig. 5. TG curves for composites with (a) P-MMT and (b) Na-MMT. (Δ*m*) Loss of mass and (*T*) temperature; the same for Fig. 6. (*1*) PE, (*2*) PE/MAPE, (3) PE/MMT, and (*4*) PE/MAPE/MMT.

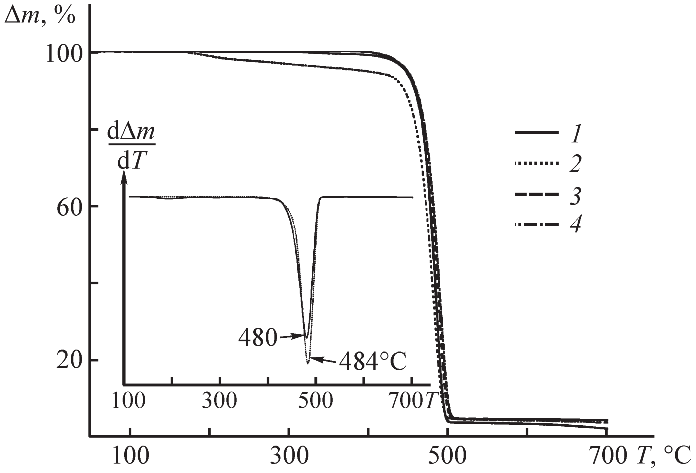

Fig. 6. TG curves for composites (*1*) PE, (*2*) MAPE, (*3*) PE/P-MMT, and (*4*) PE/MAPE/P-MMT. The inset shows DTG curves for the polymers: (*1*) PE and (*2*) MAPE.

the formation of exclusively unoxidized low-molecular saturated and unsaturated hydrocarbons. It can be seen in the TG curves in Fig. 6 that aluminosilicate particles do not exhibit the due activity under the given thermal destruction conditions.

Additional presence of oxygen-containing groups in the polymer structure (as, e.g., in MAPE) makes a particular contribution to the origination of oxidation processes. In turn, phosphorus in a phosphorus-containing modifier inhibits (via binding of $HO^\bullet$ and $HOO^\bullet$ radicals) radical reactions occurring in the polymer at high temperatures. It has been found [44] that the destruction of the phosphonium salt (accelerated under the action of acid-base centers of the layered aluminosilicate and residual anions of the salt itself) occurs to give phosphines and phosphites by the Scheme 1.

In contrast to the destruction of the salt itself, the phosphonium cation in the modified MMT decomposes to give, in addition to alkanes, alkenes, and triphenylphosphine, also triphenylphosphine oxide [$(C_6H_5)_3PO$] and *n*-aliphatic aldehydes. Thus, mostly reactions 1, 2, and 4 (Scheme 1) occur in the destruction of the modified MMT. In this case, both the number of isomers and the number of derivatives of aromatic and unsaturated aliphatic compounds grow with temperature increasing within the range 250–400°C on the background of the continuous formation of $(C_6H_5)_3P$ and $(C_6H_5)_3PO$.

To confirm the aforesaid, Table 4 list values of the coke number, obtained upon a 2-min pyrolysis of polymers and composites on their basis at a temperature of 850°C. The comparatively large values of the coke

Scheme 1.

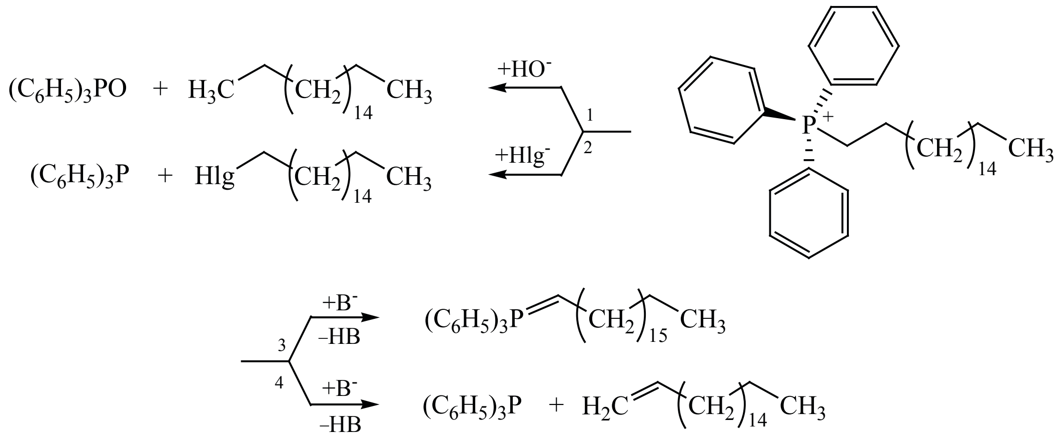

number (up to 4 and 7 wt %) are characteristic of the nanocomposite and microcomposite with P-MMT (sample nos. 4 and 5).

Being a macromolecular hydrocarbon, polyethylene is a fire-hazardous material. Its combustion begins even at an oxygen concentration of 17–18 vol % (the content of oxygen in air is 20–21 vol %) [45], its firing time does not exceed 10 s, and it occupies a leading position in the maximum rate of heat release in combustion (800–200 kW m^{-2}) [33, 46] among most of polymers. Filling of polyethylene with mineral fire-retarding agents of the $Mg(OH)_2$, $Al_2O_3 \cdot 3H_2O$, $ZnO \cdot B_2O_5 \cdot H_2O$ type, whose content may be as high as 60–80 wt %, and occasionally even more than 100 wt % (with the oxygen index not exceeding 20 vol % at low concentrations), can raise the OI of he material to 25–27 vol % at the expense of its other properties [47–49]. Use of more effective, but, at the same time, also more toxic halogen-containing fire-retardants, e.g., decabromodiphenyl oxide or chlorinated paraffin, or their joint application with antimony [Sb(II) and Sb(V)] compounds as synergists [50, 51] entails risk of poisoning by their destruction products both in processing and in combustion of a filled material [52].

Montmorillonite is widely recognized as available and inexpensive native filler and fire-retardant [53] with physical mode of functioning [53]. The certain type of structure formed in the PE/MMT nanocomposite in the course of extrusive mixing exerts a certain influence on the heat balance of the combustion process. In this case, the polymeric material having an enhanced thermal stability resists inflammation during a substantially longer time. To improve the fire resistance of the composites, montmorillonite was treated with a phosphorus-containing modifier whose content was 29 wt % in MMT, or 0.8 wt % in the composite. The phosphorus compounds formed in the thermal destruction [$(C_6H_5)_3PO$, $(C_6H_5)_3P$] decompose in the pyrolysis zone to give active species of the type of P_2, PO, PO_2 (and, to a lesser extent, P and HPO) by the scheme

$$\mathrm{P^{\cdot} + HOO^{\cdot} \rightarrow PO_2^{\cdot} + H,}$$
$$\mathrm{P + HO^{\cdot} \rightarrow PO^{\cdot} + H,}$$
$$\mathrm{HO^{\cdot} + PO^{\cdot} \rightarrow HPO^{\cdot} + O^{\cdot},}$$
$$\mathrm{HPO^{\cdot} + H^{\cdot} \rightarrow H_2 + PO^{\cdot}.}$$

Radicals of this type are mostly important in the preflame zone [54].

Table 4 presents the results obtained in tests of the composites by the oxygen index (OI) method and those for the flame propagation rate parameter ν. For example, the OI of microcomposites with Na-MMT or P-MMT is comparable with that of unfilled polyethylene. However, the nanocomposite exhibits a slower combustion because of the formation of intercalated and exfoliated structures (compare values of ν for sample nos. 3 and 7 with those for no. 5). In this case, a comparatively large OI (20 vol %) is characteristic of the nanocomposite with P-MMT, based on the polymer-polymer mixture. It is noteworthy that, being a synergist when combined with halogen-free fire-retarding agents, organomontmorillonite (in which the modifier is more thermally stable than ammonium salts and tends to inhibit combustion) makes it possible to significantly raise the fire resistance of polyethylene [56–58].

The melt flow index (MFI) of microcomposite nos. 4 and 6 does not differ from that of the unfilled polymer. The adhesion interactions (enhanced upon an increase in the degree of exfoliation due to the formation of a highly developed specific surface area) between maleic anhydride grafted to the polymer and active centers of the layered aluminosilicate and the particle orientation in the polymer bulk [59] lead to a decrease in OI and increase in the melt viscosity both for the base PE/MAPE composition and for the nanocomposite with P-MMT and microcomposite with Na-MMT (Table 4; sample nos. 3, 5, and 7). The decrease MFI is also due to the high viscosity of the molten MAPE itself, whose high content (up to 45 wt %) of maleic anhydride makes larger the number of macromolecule entanglements in the bulk [60]. Composites of this kind can be processed by compaction or extrusion.

CONCLUSIONS

(1) The formation of nanocomposites based on linear polyethylene with montmorillonite of nanostructured morphology is governed by the presence of a compatibilizer in the composite and modifier in montmorillonite.

(2) A certain type of nanostructure fundamentally affects the barrier, stress-strain, thermal, and fire-resistance characteristics of the polymer.

(3) Intercalated and exfoliated structures formed by the aluminosilicate in the course of mixing differently affect the sorption and thermo-oxidative processes. Aluminosilicate nanoparticles favor formation of coke and make slower the rate of heat and gas penetration into the polymer, which retards its combustion.

ACKNOWLEDGMENTS

The authors express sincere gratitude to colleagues from the Institute of Chemistry, Academy of Sciences, People's Republic of China (Beijing), Prof. Y. Mingshu and Dr. W. Feng for assistance in the study and permanent attention.

REFERENCES

1. Rozengart, M.I., V'yunova, G.M., and Isagulyants, G.V., *Russ. Chem. Rev.*, 1988, Issue 2, vol. 57, p. 115.
2. Okada, A., Kawasumi, M., Usuki, A., et al., *Mater. Res. Soc. Symp. Proc.*, 1990, vol. 171, p. 45.
3. Usuki, A., Kojima, Y., Okada, A., et al., *J. Mater. Res.*, 1993, vol. 8, p. 1174.
4. Kojima, Y., Usuki, A., et al., *J. Polym. Sci. Part A,* 1993, vol. 31, p. 1755.
5. Vaia, R.A., Ishii, H., and Giannelis, E.P., *Chem. Mater.*, 1993, vol. 5, p. 1694.
6. Giannelis, E.P., *Adv. Mater.*, 1996, vol. 8, p. 29.
7. Giannelis, E.P., *Appl. Organomet. Chem.*, 1998, vol. 12, p. 675.
8. Giannelis, E.P., Krishnamoorti, R., and Manias, E., *Adv. Polym. Sci.*, 1999, vol. 138, p. 107.
9. LeBaron, P.C., Wang, Z., and Pinnavaia, T.J., *Appl. Clay Sci.*, 1999, vol. 15, p. 11.
10. Vaia, R.A., Price, G., Ruth, P.N., et al., *Appl. Clay Sci.,* 1999, vol. 15, p. 67.
11. Biswas, M. and Sinha Ray, S., *Adv. Polym. Sci.*, 2001, vol. 155, p. 167.
12. Sinha, Ray S. and Okamoto, M., *Prog. Polym. Sci.,* 2003, vol. 28, p. 1539.
13. Okamoto, M., *Mater. Sci. Tech.*, 2006, vol. 22, no. 7, p. 756.
14. Fischer, H., *Mater. Sci. Eng. C*, 2003, vol. 23, p. 763.
15. Wang, Y., Chen, F.-B., and Wu, K.-C., *J. Appl. Polym. Sci.*, 2005, vol. 97, no. 4, p. 1667.
16. Wang, K.H., Choi, M.H., Koo, Ch.M., et al., *Polymer*, 2001, vol. 42, p. 9819.
17. Durmus, A., Woo, M., Kasgoz, A., et al., *Macromol. Nanotech.,* 2007, vol. 43, p. 3737.
18. Mehrabzadeh, M. and Kamal, M.R., *Polym. Eng. Sci.,* 2004, vol. 44, no. 6, p. 1152.
19. Leszczynska, A., Njuguna, J., Pielichowski, K., and Banerjee, J.R., *Thermochim. Acta,* 2007, vol. 453, p. 75.
20. Stoeffler, K., Lafleur, P.G., and Denault, J., *Polym. Eng. Sci.,* 2008, vol. 48, no. 8, p. 1449.
21. Xiao, W., Zhan, M., and Li, Z., *Mater. Des.*, 2003, vol. 24, no. 6, p. 455.
22. Moraru, V.N., *Appl. Clay Sci.*, 2001, vol. 19, p. 11.
23. Pozsgay, A., Frater, T., Szazdi, L., et al., *Eur. Polym. J.,* 2004, vol. 40, p. 27.
24. Bakhov, F.N., Cad. Sci. Dissertation, Moscow, 2007.
25. Lyatskaya, Y. and Balazs, A.C., *Macromolecules,* 1998, vol. 31, p. 6676.
26. Balazs, A.C., Singh, C., Zhulina, E., and Lyatskaya, Y., *Acc. Chem. Res.*, 1999, vol. 32, p. 651.
27. Ginzburg, V.V. and Balazs, A.C., *Macromolecules*, 1999, vol. 32, p. 5681.
28. Ginzburg, V.V., Singh, C., and Balazs, A.C., *Macromolecules*, 2000, vol. 33, p. 1089.
29. Ginzburg, V.V., *Macromolecules*, 2005, vol. 38, p. 2362.
30. Morawiec, J., Powlak, A., Slouf, M., et al., *Eur. Polym. J.*,

2005, vol. 41, p. 1115.

31. Hotta, S. and Paul, D.R., *Polymer,* 2004, vol. 45, p. 7639.
32. Zhao, C., Qin, H., Gong, F., et al., *Polym. Degrad. Stab*., 2005, vol. 87, p. 183.
33. Zhang, J. and Wilkie, Ch.A., *Polym. Degrad. Stab.,* 2003, vol. 80, p. 163.
34. Dolgov, V.V., Ashurov, N.R., Sadykov, Sh.G., and Usmanova, M.M., *Uzbek. Khim. Zh.,* 2012, no. 2, p. 30.
35. Dolgov, V.V., Ashurov, N.R., Sadykov, Sh.G., and Usmanova, M.M., *Uzbek. Khim. Zh.,* 2012, no. 1, p. 3.
36. Tolle, T.B. and Anderson, D.P., *Compos. Sci. Tech.*, 2002, vol. 62, p. 1033.
37. Ashurov, N.R., Sadykov, Sh.G., and Dolgov, V.V., *Polym. Sci. Ser. A*, 2012, vol. 54, no. 9, p. 724.
38. Arunvisut, S., Phummanee, S., and Somwangthanaroj, A., *J. Appl. Polym. Sci*., 2007, vol. 106, p. 2210.
39. Gorrasi, G., Tortora, M., Vittoria, V., et al., *Polymer,* 2003, vol. 44, p. 3679.
40. Kovaleva, N.Yu., Brevnov, P.N., Grinev, V.G., et al., *Vysokomol. Soedin., Ser. A*, 2004, vol. 46, no. 6, p. 1.
41. Reitlinger, S.A., *Pronitsaemost' polimernykh materialov* (Permeability of Polymeric Materials), Moscow: Khimiya, 1974.
42. Bershtein, V.A. and Egorov, V.M., *Differentsial'naya skaniruyushchaya kalorimetriya v fizikokhimii polimerov* (Differential Scanning Calorimetry in Physical Chemistry of Polymers), Leningrad: Khimiya, 1990.
43. Novokshonova, L.A., Brevnov, P.N., Grinev, V.G., et al., *Ros. Nanotekhnol*., 2008, vol. 3, nos. 5-6, p. 136.
44. Xie, W., Xie, R., Pan, W.-P., et al., *Chem. Mater.,* 2002, vol. 14, p. 4837.
45. Vasile, C. and Pascu, M., *Practical Guide to Polyethylene,* Shawbury: Smithers Rapra Press, 2008, p. 188.
46. Wang, S., Hu, Y., Zhongkai, Q., et al*., Mater. Lett*., 2003, vol. 57, p. 2675.
47. Yeh, J.T., Yang, H.M., and Huang, S.S., *Polym. Degrad. Stab.,* 1995, vol. 50, p. 229.
48. Yeh, J.T., Yang, M.J., and Hsieh, S.H., *Polym. Degrad. Stab*., 1998, vol. 61, p. 465.
49. Zhang, X., Guo, F., Chen, J., et al., *Polym. Degrad. Stab*., 2005, vol. 87, p. 411.
50. Kyazimova, T.G., Babaev, R.S., Dzhafarov, A.S., and Mamedova, E.S., *Plast. Massy,* 1977, no. 12, p. 38.
51. Meshkova, I.N., Petrosyan, A.I., Lalayan, V.M., and Dubnikova, I.L., *Polym. Sci.,* 2008, Ser. B, vol. 50, no. 5, p. 111.
52. Ebert, J. and Bahadir, M., *Environment Int*., 2003, vol. 29, p. 711.
53. Laoutid, F., Bonnaud, L., Alexandre, M., et al., *Mater. Sci. Eng. R,* 2009, vol. 63, p. 100.
54. Hastie, J.W.*, Res. Nat. Bur. Stand. A*, 1973, vol. 77, no. 6, p. 733.
55. Huang, G., Li, Y., Han, L., et al., *Appl. Clay Sci.,* 2011, vol. 51, p. 360.
56. Chang, Z.-H., Guo, F., Chen, J.-F., et al., *Polymer*, 2007, vol. 48, p. 2892.
57. Zhang, J., Jiang, D.D., and Wilkie, Ch.A., *Polym. Degrad. Stab*., 2006, vol. 91, p. 298.
58. Zhang, J. and Wilkie, Ch.A., *Polym. Adv. Technol*., 2005, vol. 16, p. 549.
59. Drozdov, A.D., Jensen, E.A., and Christiansen, J. de C., *Comput. Mat. Sci.,* 2008, vol. 43, p. 1027.
60. Gaylord, N.G., Mehta, R., Mohan, D.R., and Kumar, V., *J. Appl. Polym. Sci.,* 1992, vol. 44, p. 1941.